Monatshefte für Chemie 129, 1103–1117 (1998)

Monatshefte für Chemie
Chemical Monthly

Electrochemical Behaviour of a Silver Electrode in NaOH Solutions

Sayed S. Abd El Rehim*, **Hamdy H. Hassan, Magdy A. M. Ibrahim,** and **Mohammed A. Amin**

Faculty of Science, Ain Shams University, Cairo, Egypt

Summary. Studies of the electrochemistry of metals and alloys are very important fields of scientific and industrial work. The present investigation includes detailed studies on the corrosion and electrochemical behaviour of Ag in aqueous NaOH solutions under various conditions using cyclic voltammetry, chronoamperometry, and potentiostatic techniques. It was found that the anodic polarization curve of Ag in NaOH solutions is characterized by the occurrence of five anodic peaks (*A1–A5*). *A1* is due to the electroformation of soluble $[Ag(OH)_2]^-$ complex species, *A2* to the electroformation of Ag_2O, *A3* to nucleation and three dimensional growth of the Ag_2O layer, *A4* to the formation of AgO, and *A5* presumably to the formation of Ag_2O_3. X-ray diffraction patterns confirmed the existence of passive Ag_2O and AgO layers on the electrode surface potentiodynamically polarized up to oxygen evolution.

The cathodic part of the cyclic voltammograms is characterized by the occurrence of an activated anodic peak (*A6*) corresponding to the electrooxidation of Ag to Ag_2O and three cathodic peaks (*C1*, *C2*, *C2′*) corresponding to the electroreduction of AgO to Ag_2O and Ag_2O to Ag, respectively.

Keywords. Cyclic voltammetry; Silver electrode; Alkaline solutions.

Elektrochemisches Verhalten einer Silberelektrode in Natriumhydroxidlösungen

Zusammenfassung. Die Elektrochemie von Metallen und Legierungen stellt ein wichtiges Arbeitsgebiet in Forschung und Industrie dar. Die hier vorgestellte Untersuchung beinhaltet detaillierte Studien zur Korrosion und zum elektrochemischen Verhalten von Silber in wäßrigen Natriumhydroxidlösungen mittels cyclischer Voltammetrie, Chronoamperometrie und potentiostatischer Techniken. Die anodische Polarisationskurve von Ag in NaOH wird durch das Auftreten von fünf anodischen Peaks (*A1–A5*) charakterisiert. *A1* resultiert aus der elektrochemischen Bildung von löslichen komplexen Species des Typs $[Ag(OH)_2]^-$, *A2* aus jener von Ag_2O, *A3* geht auf Keimbildung und dreidimensionales Wachstum der Ag_2O-Schicht zurück, *A4* auf die Bildung von AgO, und *A5* wird vermutlich durch die Bildung von Ag_2O_3 verursacht. Röntgendiffraktionsmuster bestätigen die Existenz passiver Ag_2O- und AgO-Schichten an der Elektrodenoberfläche bei potentiodynamischer Polarisation bis zur Wasserstoffentwicklung.

Der kathodische Teil der cyclischen Voltammogramme wird durch einen aktivierten anodischen Peak (*A6*, entsprechend der Elektrooxidation von Ag zu Ag_2O) und drei kathodische Peaks (*C1*, *C2*, *C2′*, entsprechend der Elektroreduktion von AgO zu Ag_2O und von Ag_2O zu Ag) charakterisiert.

* Corresponding author

Introduction

The anodic behaviour of Ag in alkaline solutions has been extensively studied, mainly due to the use of silver electrodes in various types of alkaline and sea water batteries and the nucleation and growth of AgO on Ag/Ag_2O substrates serving as cathodes in Ag-Zn alkaline rechargeable batteries [1–3].

The anodic oxidation of Ag metal in alkaline solution proceeds *via* a two-step mechanism [4, 5]. The first step is the oxidation of Ag to Ag_2O which is supposed to be a diffusion controlled reaction, the diffusion control being established in the solid phase [6]. The growth of the silver oxide layer under linear potential sweep or potential step measurements has been shown to involve as a first step the formation of Ag_2O or AgOH monolayers at potentials close to the Ag/Ag_2O reversible electrode potential. These monolayers grow through a solid diffusion mechanism to form a 3-D primary silver(I) oxide.

The second oxidation step is the oxidation of Ag_2O to AgO which proceeds *via* nucleation and crystal growth processes [7, 8]. The cyclic voltammograms (CVs) obtained by *Dirkse et al*. [4] suggested that one of the latter processes is slow and that the CV peak associated with it appears only at slow sweep rates. *Salvarezza et al*. [9] have investigated the electroformation of an Ag(II) oxide layer during the anodization of silver in 0.1 *M* NaOH under potentiostatic and potentiodynamic conditions. Results are discussed in terms of nucleation and growth models and statistical analysis of induction times related to the nucleation kinetics of Ag(II) oxide crystals. *Hepel et al*. [3] have obtained cyclic voltammograms for the polycrystalline smooth silver electrode that consist of five anodic peaks of which only two are associated with the formation of bulk Ag_2O and Ag_2O_2. According to *Brezina et al.* [10], the multilayer surface oxides are formed in the region of the first oxidation peak, whereas *Giles et al.* [11, 12] have proposed that a monolayer of Ag_2O is completed in the region of the first oxidation peak. Based on a ring-disc study, *Ambrose* and *Barradas* [13] have concluded that dissolution of silver(I) as $[Ag(OH)_2]^-$ occurs in the region of the first oxidation peak. From combined electrochemical and ellipsometric studies, *Droog et al.* [14], have proposed that the first oxidation peak is due to silver dissolution and the formation of a surface monolayer. *Burstein et al.* [15] have demonstrated that there will be at least three well defined peaks, a fact which suggests that the formation of Ag(I) oxide is a multistage process; they assigned the first stage to the electroformation of a monolayer of either Ag_2O or AgOH and the second stage to the electroformation of either a base Ag_2O layer or an O-layer trapped in the Ag surface (O-Ag alloy) or to Ag electrodissolution as $[Ag(OH)_2]^-$. Finally, the third stage of Ag_2O electroformation which corresponds to the last anodic current peak has been assigned to the 3-D growth of the Ag_2O phase.

Very little work has been published on the cyclic voltammetric behaviour of Ag in alkaline media between hydrogen and oxygen evolution potentials, the topic upon which this investigation is focused. The influence of various parameters including potential scan limit, scan rate, electrolyte concentration, solution temperature, and repetitive cycling on the voltammetric behaviour of Ag electrode was studied.

Results and Discussion

Cyclic voltammetric behaviour of silver electrodes in NaOH solutions

Figure 1 shows a typical first cyclic voltammetric scan of an Ag electrode in 1.0 *M* NaOH at 25°C between $E_{s,c} = -1680\,\text{mV}$ and $E_{s,a} = 900\,\text{mV}$ at a scan rate of $100\,\text{mV} \cdot \text{s}^{-1}$. This voltammogram is consistent with those published previously [1–5]. The anodic excursion span characterized by five anodic current peaks (two major ones (*A3* and *A4*) and three minor ones (*A1*, *A2* and *A5*)) prior to oxygen evolution potential. The reverse potential scan exhibits an activated anodic current peak (*A6*) and three cathodic contributions (*C1*, *C2*, and a small cathodic shoulder (*C2′*)) prior to hydrogen evolution potential.

According to a literature review [1, 13, 16], the first small anodic peak (*A1*) might be related to the electrodissolution of Ag to $[Ag(OH)_2]^-$ through adsorption of OH^- and desorption and diffusion of soluble $[Ag(OH)_2]^-$:

$$Ag + 2OH^-_{ads} \rightleftharpoons [Ag(OH)_2]^-_{ads} + e^-$$
$$[Ag(OH)_2]^-_{ads} \rightleftharpoons [Ag(OH)_2]^-_{aq}$$

On the other hand, the second anodic current peak (*A2*) could be attributed to the electroformation of a monolayer of Ag_2O resulting from the precipitation of $[Ag(OH)_2]^-$ from its supersaturated solution at the electrode surface as confirmed by optical studies [16, 17]. *Giles et al.* [11] have shown that the formation of a

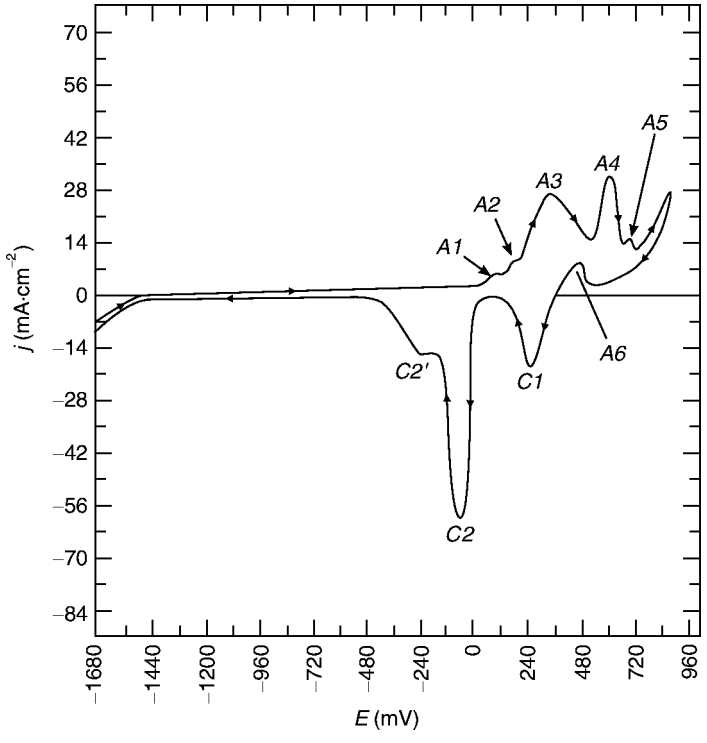

Fig. 1. Typical first cyclic voltammetric scan for a polycrystalline Ag electrode in 1.0 *M* NaOH between $E_{s,c} = -1680\,\text{mV}$ and $E_{s,a} = 900\,\text{mV}$ at 25°C and $100\,\text{mV} \cdot \text{s}^{-1}$

monolayer of Ag_2O slows down the rate of anodic dissolution and the formation of $[Ag(OH)_2]^-$.

The anodic current peak *A3* can be ascribed to the thickening of the completed basal monolayer, *i.e.* the electroformation of a multilayer of Ag_2O. Recently it has been reported that the thickening process occurs *via* a nucleation and growth mechanisms [15, 17, 18] according to

$$2Ag + 2OH^- \rightleftharpoons Ag_2O + H_2O + 2e^-$$

The anodic peak *A4* is due to the electrooxidation of Ag_2O and the formation of AgO according to the overall chemical reaction [1, 2, 19]

$$Ag_2O + 2OH^- \rightleftharpoons 2AgO + H_2O + 2e^-$$

In addition, it is possible that direct electrooxidation of Ag to AgO occurs within the potential range of peak *A4* [7–20]:

$$Ag + 2OH^- \rightleftharpoons AgO + H_2O + 2e^-$$

X-ray diffraction analyses of the oxidation products formed on the surface of the Ag anode polarized potentiodynamically in 1.0 *M* NaOH at 25°C at a scan rate of $100\,mV \cdot s^{-1}$ were performed at two specific polarization potentials (E_{PA3}, E_{PA4}). Spectra of the specimen polarized in the potential range of peak *A3* indicate the presence of Ag_2O, whereas those of the specimen polarized in the potential range of peak *A4* confirm the existence of AgO and traces of Ag_2O, thus supporting the conclusion that some of the charge accepted by the electrode may contribute to thicken or to form new Ag_2O in this potential range [3].

The small anodic peak *A5* which appears just prior to oxygen evolution potential might be correlated to the electroformation of the highest silver oxide, Ag_2O_3, as has been reported in Refs. [17, 21–24]:

$$2AgO + 2OH^- \rightleftharpoons Ag_2O_3 + H_2O + 2e^-$$

On the other hand, the existence of anodic peak *A6* at the revers scan in the potential range of peak *A3* could be attributed to continuous nucleation and growth of an Ag_2O film as a result of electrooxidation of the basal Ag metal [2].

The cathodic peak *C1* is ascribed to the electroreduction of AgO to Ag_2O according to

$$2AgO + H_2O + 2e^- = Ag_2O + 2OH^-,$$

indicating that this peak is conjugated to the anodic peak *A4*. On the other hand, the more negative cathodic peaks *C2* and *C2′* could be related to processes involved in electroreduction of Ag(I) oxygen species. One of the points of disagreement in the published literature is the presence or absence of the cathodic shoulder *C2′* which has not been observed in all previous investigations. Its appearance indicates the complex nature of Ag_2O electroreduction.

Effect of anodic potential scan limit

The complementary relationship between the anodic and cathodic current peaks of an Ag electrode can be established more clearly by increasing the anodic limiting potential $E_{s,a}$ stepwise. Figure 2 shows the first cyclic voltammetric scan for an Ag

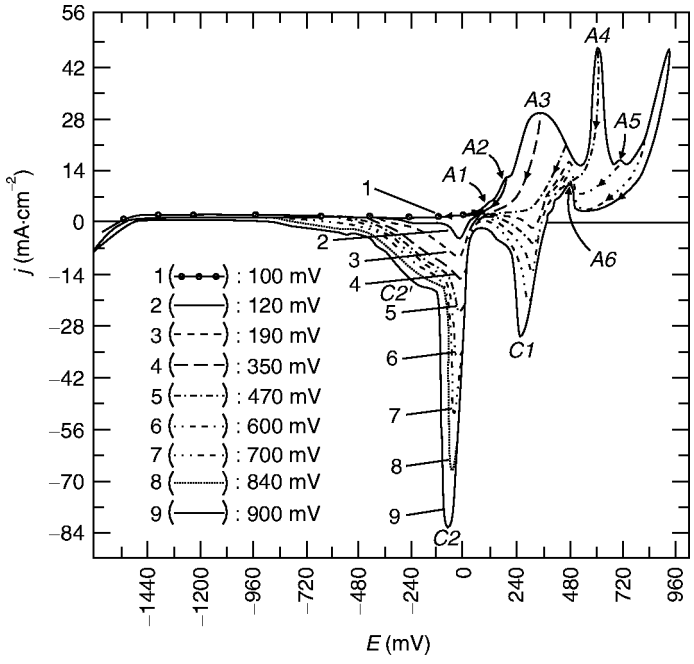

Fig. 2. Typical first cyclic voltammetric scan for polycrystalline a Ag electrode in 1.0 *M* NaOH at 25°C at a scan rate of $100\,\mathrm{mV}\cdot\mathrm{s}^{-1}$, starting from $E_{s,c} = -1680\,\mathrm{mV}$ and being reversed at various anodic potentials

electrode in 1.0 *M* NaOH at 25°C. The measurement starts at $E_{s,c} = -1680\,\mathrm{mV}$ and is reversed at various anodic potentials $E_{s,a}$ with a scan rate of $100\,\mathrm{mV}\cdot\mathrm{s}^{-1}$. If $E_{s,a}$ is reversed at a potential more negative than the peak potential of peak *A1* (*i.e.* at $E_{s,a} = 100\,\mathrm{mV}$), the reverse potential scan retraces itself and does not display any cathodic peaks, indicating that the anode surface is free from any passive layers. When the anodic potential is reversed within the potential range of peak *A1* (*i.e.* at $E_{s,a} = 120\,\mathrm{mV}$), the reverse scan retraces part of the forward scan and then yields the cathodic peak *C2* with its shoulder *C2′*, indicating that these peaks are correlated to the electroreduction of the Ag_2O film to Ag. When the anodic potential is reversed at a potential more positive than that of peak *A2* (*i.e.* at $E_{s,a} = 200\,\mathrm{mV}$), hysteresis between the forward and the return scan is observed prior to the appearance of the cathodic peaks *C2* and *C2′* indicating that the anode surface becomes completely covered with a resistive Ag_2O passive layer. When the anodic potential limits are reversed within the potential range of peak *A3*, the reversed scans yield the cathodic peaks *C2* and *C2′*. A stepwise increase of $E_{s,a}$ causes the heights of peaks *C2* and *C2′* to increase and shifts their peak potentials to more negative values. It seems probable that an increase in the anodic potential limit enhances the stability and protective ability of the Ag_2O layer, presumably as a result of increasing its thickness.

If the anodic potential is reversed at $E_{s,a} = 470\,\mathrm{mV}$ (between the end of peak *A3* and the beginning of peak *A4*), the reverse scan is characterized by the appearance of the activated anodic peak *A6*. The cathodic half cycle displays three cathodic

peaks *C1*, *C2*, and *C2′*. The appearance of the cathodic peak *C1* is related to the electroreduction of AgO to Ag_2O; therefore, its appearance indicates that the anodic peak *A4* is due to the formation of AgO film. It is worth mentioning that a further stepwise increase in the anodic potential limit up to oxygen evolution potential results in the formation of the three cathodic peaks mentioned above as well; their heights, however, increase, and their peak potentials shift towards more negative potentials with increasing potential scan limit.

Effect of potential scan rate

The effect of the potential scan rate on the first cyclic *E/j* response of an Ag electrode in 1.0 *M* NaOH at 25°C between hydrogen and oxygen evolution potentials was examined; the results are depicted in Fig. 3. It is obvious that, except for *A4* and *A5*, all peaks become more negative with increasing scan rate. The data reveal that the peak current densities j_p of all anodic and cathodic peaks increase with increasing scan rate. The relations between j_p and $\nu^{1/2}$ for both the anodic and cathodic peaks are given in Fig. 3b; straight lines passing through the origin are observed except for *A3* and *A4*. The linear relations indicate that the formation and reduction of Ag_2O are diffusion controlled processes.

For a diffusion controlled process under potentiodynamic conditions, the slopes of j_p *vs.* $\nu^{1/2}$ are proportional to the concentration of the diffusing species (c) and to the square root of their diffusion coefficients (D) according to the following equation [25] where a and b are constants and z is the number of exchanged electrons.

$$j_p = a \cdot b \cdot z^{1/2} \cdot c \cdot D^{1/2} \cdot \nu^{1/2}$$

However, it seems that the peak current dependence of *A4* on the scan rate is superimposed by the current related to peak *A3*, making it difficult to obtain the separated dependence of *A4*. In this case, the relationship between j_p and $\nu^{1/2}$ for peak *A4* suggests a surface process which is not purely diffusion controlled.

Effect of NaOH concentration

The effect of NaOH concentration (0.1 to 2.0 *M*) on the first cyclic voltammetric scan of an Ag electrode between hydrogen and oxygen evolution potentials at 25°C and a scan rate of $100\,mV \cdot s^{-1}$ was examined; the results are given in Fig. 4. Inspection of the data reveals that the rates of both hydrogen and oxygen evolution reactions are enhanced by increasing the NaOH concentration. Also, the charge involved in the electroformation of the oxide layer increases with increasing alkali concentration. The anodic and cathodic peak current densities increase with increasing NaOH concentration as can be seen from the linear relation between $\log j_p$ and $\log c_{NaOH}$ (Fig. 5). The anodic and cathodic peak potentials shift slightly to more negative values. The effects caused by increasing NaOH concentration can be interpreted on the basis of enhanced solubilities of silver oxides at increased alkali concentration [26].

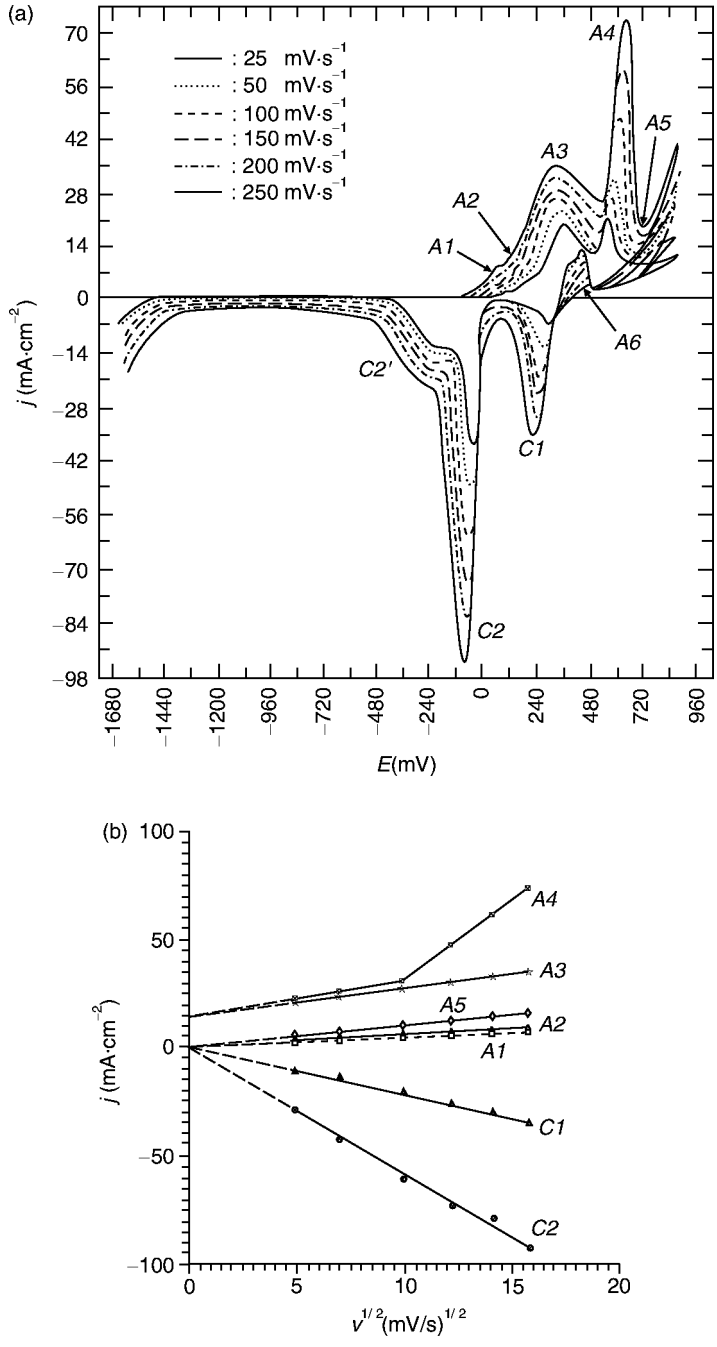

Fig. 3. a) Typical first cyclic voltammetric scan for a polycrystalline Ag electrode in 1.0 *M* NaOH between $E_{s,c} = -1680$ mV and $E_{s,a} = 900$ mV at 25°C and different scan rates; **b)** dependence of the peak current density on the square root of the potential scan rate for an Ag electrode in 1.0 *M* NaOH at 25°C

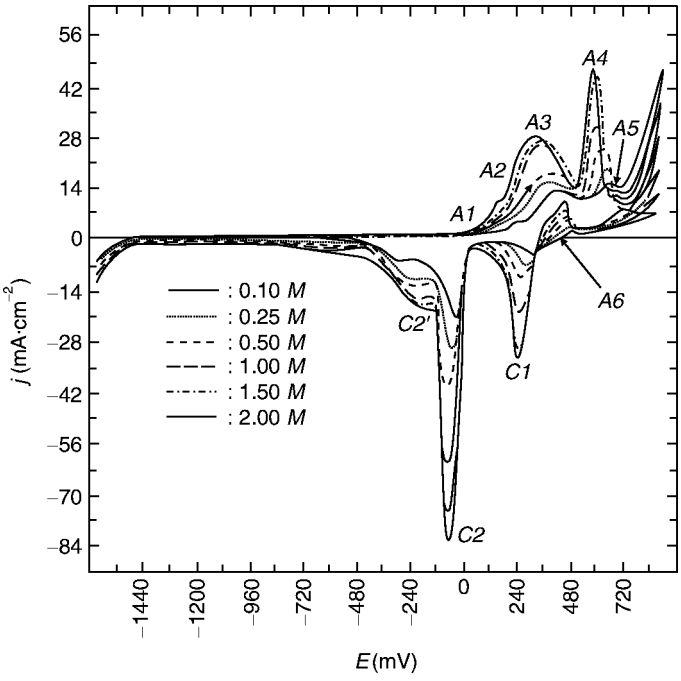

Fig. 4. Typical first cyclic voltammetric scan for a polycrystalline Ag electrode in NaOH solutions of various concentrations (0.10–2.0 *M*) between $E_{s,c} = -1680$ mV and $E_{s,a} = 900$ mV at 25°C and 100 mV · s^{-1}

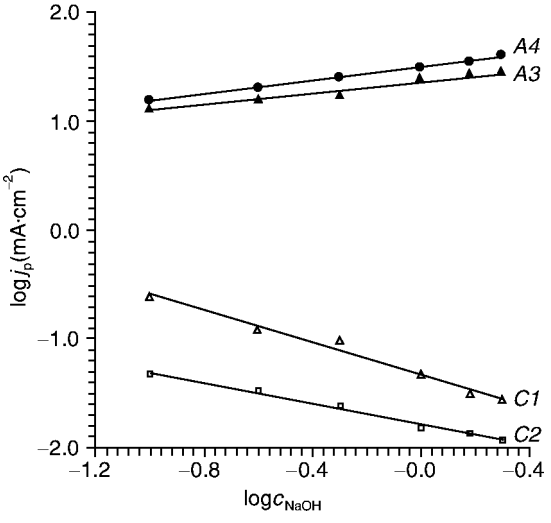

Fig. 5. Dependence of $\log j_p$ on $\log c_{NaOH}$ for an Ag electrode in NaOH solutions of various concentrations at 25°C and 100 mV · s^{-1}

Effect of temperature

Figure 6 illustrates the influence of temperature (15–75°C) on the first voltammetric scan of an Ag electrode in 1.0 *M* NaOH at a scan rate of 100 mV · s^{-1}. The general shape of the *E*/*j* response remains partially unaffected by

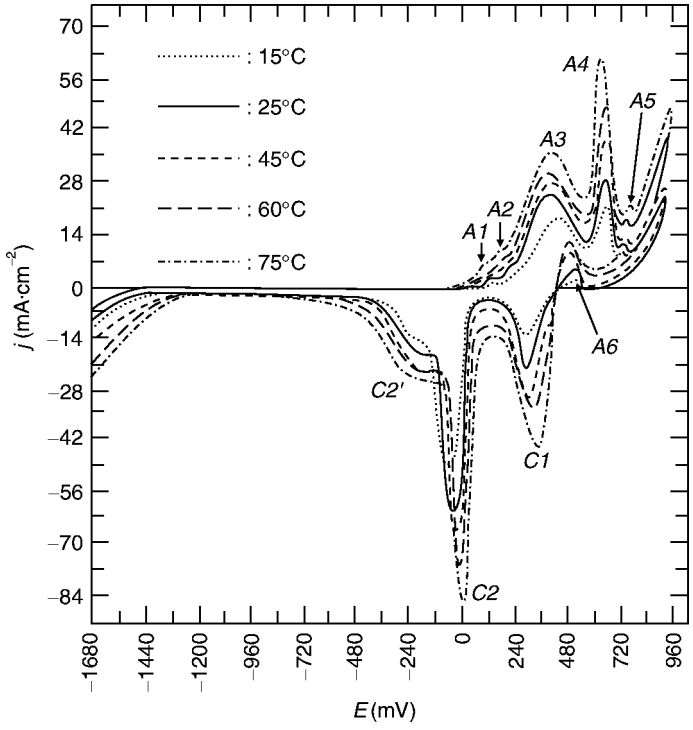

Fig. 6. Typical first cyclic voltammetric scan for a polycrystalline Ag electrode in 1.0 *M* NaOH at different temperatures (15–75°C) between $E_{s,c} = -1680\,\text{mV}$ and $E_{s,a} = 900\,\text{mV}$ at $100\,\text{mV} \cdot \text{s}^{-1}$

changing the temperature. However, the overpotentials of both hydrogen and oxygen evolution reactions decrease with increasing temperature. The rise of temperature enhances the heights of the anodic and cathodic peaks. At the same time, the peak potentials of the anodic peaks shift to more negative values, whereas those of the cathodic peaks shift towards more positive values. The stimulating effect of temperature with respect to the formation of silver oxides could be attributed to the increased solubilities of these oxides at elevated temperatures. In addition, an increase in temperature leads to higher values of the diffusion coefficients.

Effect of repetitive cycling

The influence of the number of repetitions on the general features of the voltammogram of an Ag electrode in 1.0 *M* NaOH at 25°C and $100\,\text{mV} \cdot \text{s}^{-1}$ between hydrogen and oxygen evolution potentials is shown in Fig. 7. The results infer that marked changes are observed in the heights of the anodic and cathodic peaks upon repetitive cycling, whereas their peak potentials remain nearly unaffected. It is known that the oxidation products formed during the anodic half cycle are reduced during the cathodic half cycle. Thus, the anodic charge measured during the following anodic half cycle could be considered as a measure of the free silver surface area on which the surface film is likely to be formed. Therefore, it is possible that the surface area of the Ag electrode increases progressively with

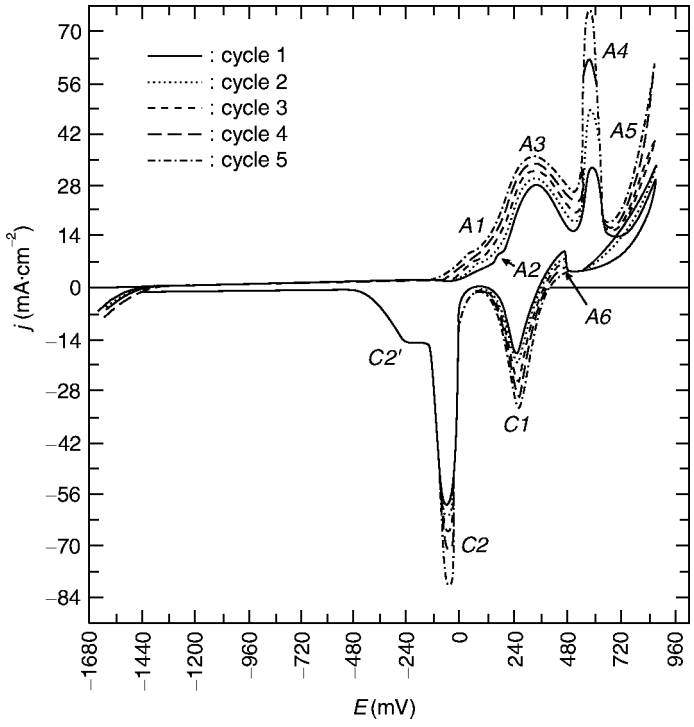

Fig. 7. Effect of repetitive cycling (5 cycles) on the *j*/*E* response of a polycrystalline Ag electrode in 1.0 *M* NaOH between $E_{s,c} = -1680$ mV and $E_{s,a} = 900$ mV at 25°C and 100 mV · s^{-1}

repetitive cycling as a result of increasing the surface roughness (*i.e.* the ratio of true surface area to apparent surface area). The increase in surface roughness can be assigned to two effects: an increase in the concentration of surface active sites and the size distribution of electrodeposition of Ag, both produced by electroreduction of the anodic film [27].

Potentiostatic current transient and stripping voltammetry

In order to gain more information about the anodic and cathodic behaviour of an Ag electrode in NaOH solution, anodic current transient and cathodic stripping voltammetric (CSV) measurements were carried out. Current transients at constant anodic step potentials $E_{s,a}$ ($200 \leq E_{s,a} \leq 730$ mV) were recorded after a two step procedure. The silver electrode was first held at $E_{s,c} = -1600$ mV for 60 seconds to attain a reproducible electroreduced silver surface; then the electrode was potentiodynamically polarized in the positive direction with a scan rate of 100 mV · s^{-1} to a step potential $E_{s,a}$ at which the current transient was recorded for 100 s (Fig. 8a). At the end of that period, the oxidation products formed on the electrode surface were reduced potentiodynamically in the same solution at a scan rate of 100 mV · s^{-1}, and the concomitant cathodic stripping voltammogram was recorded up to hydrogen evolution potential (Fig. 8b) to obtain an electroanalysis of silver oxide products.

Inspections of the data of Fig. 8 reveal that two characteristic ranges can be distinguished. For step potentials in the $200 \leq E_{s,a} \leq 620$ mV range (the Ag_2O

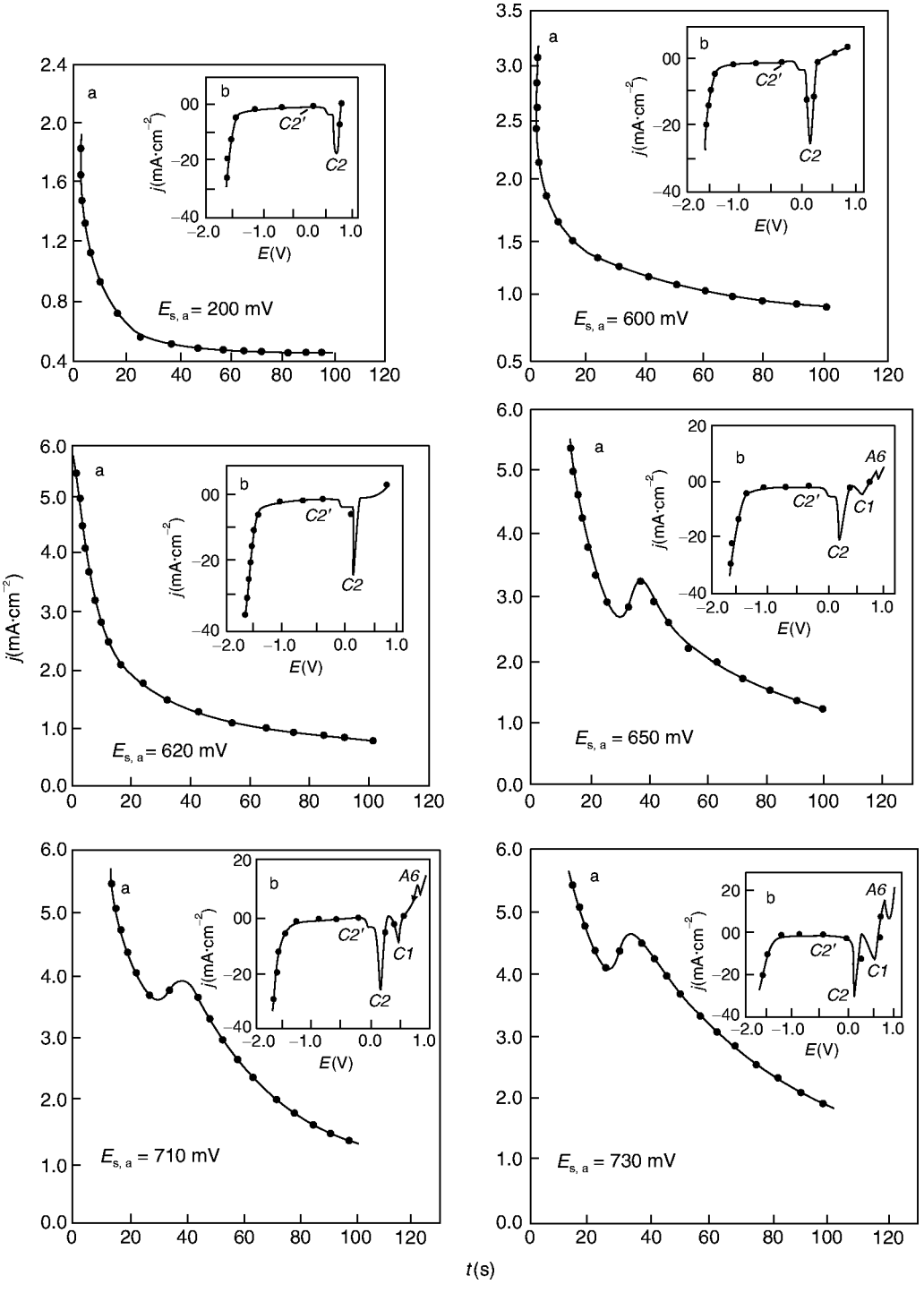

Fig. 8. a) Current transients at constant anodic step potential $E_{s,a}$ for a polycrystalline Ag electrode in 1.0 *M* NaOH at 25°C recorded at $200\,\text{mV} \leq E_{s,a} \leq 730\,\text{mV}$; **b)** cathodic stripping voltammograms at a scan rate of $100\,\text{mV} \cdot \text{s}^{-1}$ starting from $E_{s,a}$ and ending at $E_{s,c} = -1680\,\text{mV}$ after $t_s = 100\,\text{s}$

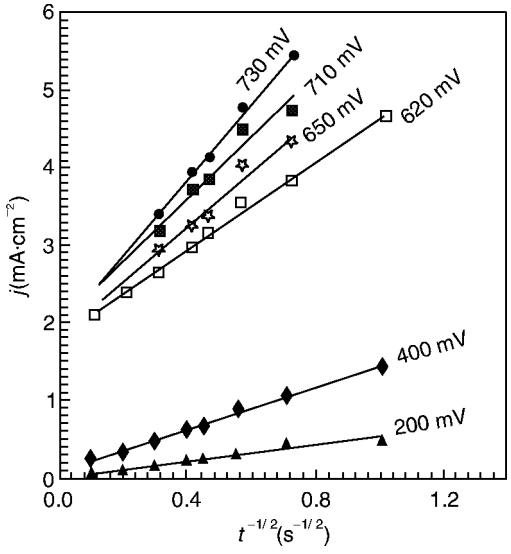

Fig. 9. Dependence of the current density on $t^{-1/2}$ for the descending portions of the current transients for an Ag electrode in 1.0 *M* NaOH at 25°C recorded in the potential range of $200\,\text{mV} \leq E_{s,a} \leq 730\,\text{mV}$

formation range), it was found that all transient currents decrease monotonically with time reaching quasi steady state current values. In this case, the transient currents are related to nucleation and growth of the Ag_2O layer. It is obvious that the corresponding stripping voltammograms (Fig. 8b) show only the cathodic peak *C2* and its shoulder *C2′*. It is obvious that the value of the quasi steady currents in the current transients (Fig. 8a) and the heights of the cathodic peaks *C2* and *C2′* (Fig. 8b) increase with increasing $E_{s,a}$, indicating an increase in the thickness of Ag_2O layer. Plotting the current $j\ vs \cdot t^{-1/2}$ for the descending parts of the current transients gives straight lines (Fig. 9). The slopes of the lines depend on the value of $E_{s,a}$. These linear relations support the suggestion that the growth of the Ag_2O layer is a diffusion controlled process and obeys the following equation [27, 28] where $P = z \cdot c \cdot D^{1/2}/\pi^{1/2}$, z is the number of exchanged electrons, c is the concentration, and D is the diffusion coefficient of the diffusing species.

$$j = P/t^{1/2}$$

On the other hand, the current transients recorded in the $650 \leq E_{s,a} \leq 730\,\text{mV}$ potential range (*i.e.* in the AgO formation range) show complicated features. The current initially decreases as a result of Ag_2O layer growth, reaching a minimum value j_m at a time t_m, then increases to reach a maximum value j_M at the time t_M, and finally decreases again and attains a quasi steady state. The rising part of the current can be attributed to partial electrooxidation of Ag_2O to AgO. It is probable that the current starts to decrease (the final decrease) again upon the formation of a more compact outer AgO layer. In this potential range, the corresponding cathodic stripping voltammograms exhibit the activated anodic peak *A6* and the two cathodic peaks *C1* and *C2* in addition to the shoulder *C2′*. The data reveal that as $E_{s,a}$ is made more positive j_m increases and both t_m and t_M decrease. Also, the

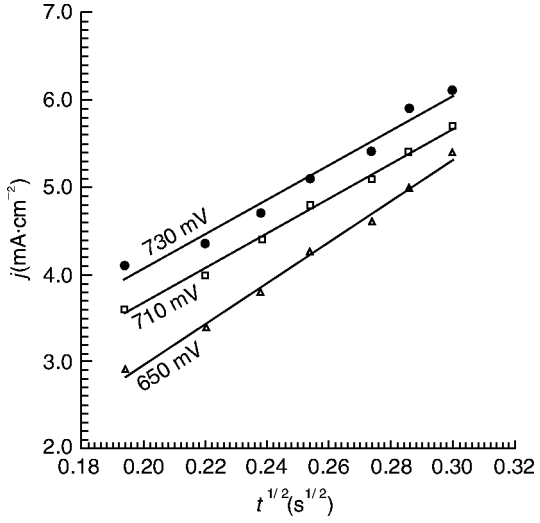

Fig. 10. Dependence of the current density on $t^{1/2}$ for the middle rising portions of the current transients for an Ag electrode in 1.0 *M* NaOH at 25°C recorded in the potential range of $650\,\text{mV} \leq E_{s,a} \leq 730\,\text{mV}$

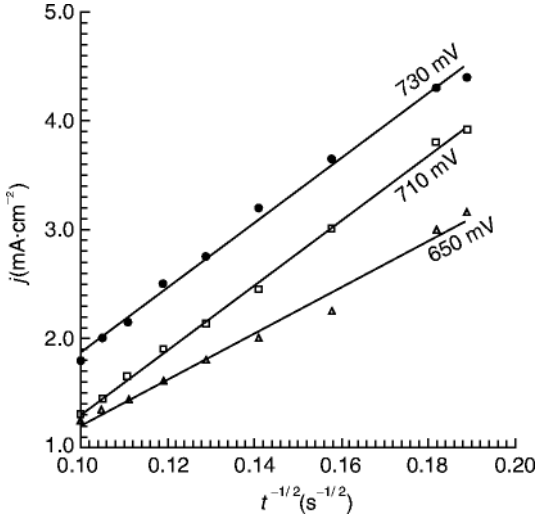

Fig. 11. Dependence of the current density on $t^{-1/2}$ for the final descending portions of the current transients for an Ag electrode in 1.0 *M* NaOH at 25°C recorded in the potential range of $650\,\text{mV} \leq E_{s,a} \leq 730\,\text{mV}$

positive shift in $E_{s,a}$ increases the heights of the two cathodic peaks *C1* and *C2* and shifts their peak potentials to more negative values. It is found that the rising parts of the transients fit the linear relation $j\ vs \cdot t^{1/2}$ shown in Fig. 10, whereas the final decreasing parts of the transients afford the corresponding graphs shown in Fig. 11. These results support the suggestion that the growth of AgO proceeds under mixed diffusion and kinetic control. Correlations between $\log j_M$ and $E_{s,a}$ as well as $\log t_M$ and $E_{s,a}$ give straight lines (data not shown). These linear relations can be taken as

an indication of a charge transfer controlled process. Therefore, these results agree with the assumption that the electrooxidation of Ag_2O to AgO in alkaline media and at high positive potentials involves a phase change for which both charge transfer and diffusion controlled growth mechanisms are responsible [29].

Experimental

The working electrode employed in the present study was made of spec pure polycrystalline silver (99.99%, Koch light laboratories, Colnbrook Bucks, England) axially embedded in an araldite holder to offer an active flat disc shaped surface of an area of $0.1256\,cm^2$. Prior to each experiment the working electrode was polished successively with fine grade emery papers. The polished metal surface was rinsed with acetone and distilled water before dipping it into the electrolytic cell. A platinum wire was used as the counter electrode. A saturated calomel electrode (SCE) was used as a reference electrode to which all potentials are referred. In order to avoid Cl^- diffusion in the cell, the reference electrode was connected to the working electrode through a bridge filled with the solution under test, the capillary tip of the bridge being pressed against the electrode to minimize the $i \cdot R$ drop. All solutions were prepared from analytical grade chemical reagents using doubly distilled water and were used without further purifications. For each run, a freshly prepared solution as well as a cleaned set of electrodes were used. Each run was carried out in aerated stagnant solution at room temperature ($25 \pm 2°C$).

Potentiodynamic polarization experiments were employed using a potentioscan type apparatus (Potentiostat, Galvanostat Model 273, EG & G). The experiments were carried out by changing the electrode potential automatically from the starting potential towards more positive values at the required scan rate till the end of the experiment. The E/j curves were recorded using an XY recorder (Omnigraphic Series 2000).

The anodic current transients at constant anodic step potentials $E_{s,a}$ within the potential range of the anodic current peaks were recorded according to a two step procedure. The silver electrode was first held at the starting potential $E_{s,c}$ for 60 s to attain a reproducible electroreduced silver surface. Then the electrode was potentiodynamically polarized in the positive direction with a scan rate of $100\,mV \cdot s^{-1}$ to a step potential $E_{s,a}$ at which the current transient was recorded for 100 s. At the end of that time, the oxidation products formed on the electrode surface were reduced potentiodynamically at the same scan rate, and the corresponding cathodic stripping voltammogram (CSV) was recorded up to hydrogen evolution potential to obtain an electroanalysis of silver oxide products.

The composition and structure of the passive film formed on the silver electrode surface was examined by X-ray diffraction analysis (Philips P. W. Model No. 1730) with Cu-K_α radiation and a nickel filter at 40 kV and 25 mA. The scanning speed was 1 degree per minute.

References

[1] Tilak BV, Perkins RS, Kozlowska HA, Conway BE (1972) Electrochim Acta **17**: 1447
[2] Stonehart P (1968) Electrochim Acta **13**: 1789
[3] Hepel M, Tomkiewicz M (1984) J Electrochem Soc **131**: 1288
[4] Dirkse TP (1990) Electrochim Acta **35**: 1445
[5] Teijelo ML, Vilche JR, Arvia AJ (1982) J Electroanal Chem **131**: 331
[6] Droog JMM, Huisman F (1980) J Electroanal Chem **115**: 211
[7] Fleischmann M, Lax DJ, Thirsk HR (1968) Trans Faraday Soc **64**: 3137
[8] Hepel M, Tomkiewciz M, Forest CL (1986) J Electrochem Soc **133**: 468
[9] Salvarezza RC, Becerra JG, Arvia AJ (1988) Electrochim Acta **33**: 1753
[10] Brezina M, Koryta J, Musilova M (1968) Coll Czech Chem Commun **37**: 3397
[11] Giles RD, Harrison JA (1970) J Electroanal Chem **27**: 161

[12] Giles RD, Harrison JA, Thirsk HR (1969) J Electroanal Chem **22**: 375
[13] Ambrose J, Barradas RG (1974) Electrochim Acta **19**: 781
[14] Droog JMM, Alderliesten PT, Bootsma GA (1979) J Electronal Chem **99**: 173
[15] Burstein GT, Newman RC (1980) Electrochim Acta **25**: 1009
[16] Perkins RS, Tilak BV, Conway BE, Kozlowska HA (1972) Electrochim Acta **17**: 1471
[17] Amlie RF, Honer HN, Ruetschi P (1965) J Electrochem Soc **112**: 1073
[18] Muller RH, Smith CG (1980) Surf Sci **96**: 375
[19] Hoar TP, Dyer CK (1972) Electrochim Acta **17**: 1563
[20] Dirkse TP, de Vries DB (1959) J Phys Chem **63**: 107
[21] Clarke TG, Hampson NA, Lee JB, Morley JR, Scanlon B (1968) Can J Chem **46**: 3437
[22] Miller B (1970) J Electrochem Soc **117**: 491
[23] Hampson NA, Mc Donald KI, Lee JB (1973) J Electroanal Chem **45**: 149
[24] Shoesmith DW, Rummery TE, Owen D, Lee W (1976) J Electrochem Soc **123**: 790
[25] Delahay P (1954) New Instrumental Methods in Electrochemistry. Wiley, New York, p 124
[26] Druskovich DM, Ritchie IM, Singh P, Guang ZH (1989) Electrochim Acta **34**: 409
[27] Randles JB (1948) Trans Faraday Soc **44**: 327
[28] Sevcik A (1948) Collect Czech Chem Commun **13**: 349
[29] Weast RC (1974–1976) Handbook of Chemistry and Physics, 55th edn. CRC Press

Received December 17, 1997. Accepted (revised) July 2, 1998